nature neuroscience

Sniffing controls an adaptive filter of sensory input to the olfactory bulb

Justus V Verhagen[1,3], Daniel W Wesson[1], Theoden I Netoff[3], John A White[2] & Matt Wachowiak[1]

Most sensory stimuli are actively sampled, yet the role of sampling behavior in shaping sensory codes is poorly understood. Mammals sample odors by sniffing, a complex behavior that controls odorant access to receptor neurons. Whether sniffing shapes the neural code for odors remains unclear. We addressed this question by imaging receptor input to the olfactory bulb of awake rats performing odor discriminations that elicited different sniffing behaviors. High-frequency sniffing of an odorant attenuated inputs encoding that odorant, whereas lower sniff frequencies caused little attenuation. Odorants encountered later in a sniff bout were encoded as the combination of that odorant and the background odorant during low-frequency sniffing, but were encoded as the difference between the two odorants during high-frequency sniffing. Thus, sniffing controls an adaptive filter for detecting changes in the odor landscape. These data suggest an unexpected functional role for sniffing and show that sensory codes can be transformed by sampling behavior alone.

Neural representations of external stimuli first occur as spatiotemporal patterns of activity across receptor neurons. Transformation of this primary receptor code is typically thought to arise from synaptic processing and anatomical reorganization in the CNS, with peripheral events having a minor role in shaping receptor coding[1,2]. For sensory modalities in which stimulus acquisition requires active sampling by the animal, sampling behavior alone has the potential to alter receptor neuron responses and the neural representation of stimulus identity. However, the extent to which sampling shapes peripheral receptor codes is not well understood.

In olfaction, odorant access to olfactory receptor neurons (ORNs) is controlled by the rhythmic inspiration and expiration of air through the nose, a process that is dependent on behavioral state[3]. For example, rodents respire at frequencies of 1–3 Hz when at rest in a familiar environment[4–6] but increase respiration to 4–12 Hz under a variety of circumstances[4,6–9]. The transition from resting respiration to active odor sampling (typically termed 'sniffing') can occur in one respiration cycle and can cease just as rapidly[5,10]. Other parameters of the respiratory cycle, such as amplitude and duration, are also heavily and rapidly modulated[7]. In odor-guided tasks performed in the laboratory, rats consistently show high-frequency sniffing at the time of odor sampling[7,8,11], and animals in a less constrained setting increase sniff frequency when tracking an odor source, scanning a substrate or investigating any novel stimulus[4,6,9]. Thus, high-frequency sniffing is presumably important in olfactory function.

Proposed roles for sniffing include increasing ORN responsiveness by increasing odorant flux into the nose[7,12], increasing the rate of odor 'snapshots' conveyed to the brain to facilitate rapid decision-making[8] and modulating ORN activity patterns to optimize the detection of particular odorants[7,13]. Sniffing also plays a critical role in olfactory information processing by imposing a rhythmic temporal structure on the input to the olfactory bulb[14–16]. Rhythmic inputs driven by sniffing are crucial for many models of olfactory bulb network function[17–19], and the timing of postsynaptic activity relative to the sniff cycle is hypothesized to encode odor information[14,20,21].

Despite the fundamental role of sniffing in olfaction, experimental data on the relationship between sniffing, odor representations and olfactory processing remain largely absent. Even a basic characterization of the response properties of ORNs during natural sniffing has not been reported in mammals. Here, we ask how sniffing shapes the mammalian receptor code for odors by imaging receptor input to the olfactory bulb in awake, head-fixed rats performing a simple odor discrimination. We imaged olfactory bulb input using calcium-sensitive dyes loaded into ORNs, a technique that yields sufficient spatial resolution to map inputs to individual glomeruli and yields a temporal resolution of tens of milliseconds[14,22]. To specifically address the role of sniffing in odor coding, we used a behavioral protocol that allowed us to compare neural representations of the same odorant sampled during low-frequency passive respiration and high-frequency sniffing.

RESULTS

Our goal was to image odorant representations during different sampling behaviors. We used a head-fixed behavioral protocol that allowed us to image receptor input to the olfactory bulb while simultaneously measuring respiration through a chronic intranasal cannula (**Supplementary Figs. 1** and **2** and **Supplementary Results** online). To ensure that the rats attended to the stimulus, we trained

[1]Departments of Biology and [2]Biomedical Engineering, Boston University, 24 Cummington Street, Boston, Massachusetts 02215, USA. [3]Current addresses: The John B. Pierce Laboratory, 290 Congress Avenue, New Haven, Connecticut 06519, USA (J.V.V.); Department of Biomedical Engineering, University of Minnesota, 312 Church St. SE NHH 7-105, Minneapolis, Minnesota 55455, USA (T.I.N.). Correspondence should be addressed to M.W. (dmattw@bu.edu).

Received 31 January; accepted 14 March; published online 22 April 2007; doi:10.1038/nn1892

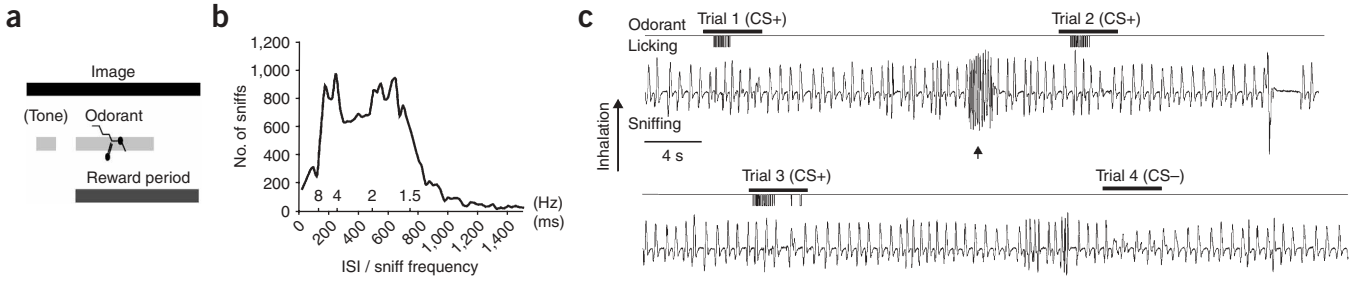

Figure 1 Sniffing behavior during head-fixed odor discriminations. (**a**) Schematic of two-odor discrimination task. Rats received a water reward for licking in response to one odorant (CS+) but not to others (CS–). In four of seven rats, a 1-s tone preceded odorant onset by 1 s. (**b**) Intersniff interval (ISI) distribution for rats performing the discrimination task. Data are from all sniffs in one session each from four rats (24,492 sniffs). Time bins are 25 ms. (**c**) Example of behavior during head-fixed odor discriminations, over four consecutive trials. Trace shows a continuous intranasal pressure measurement from one rat through four odor discriminations (100 s total time). Bars indicate presentations of CS+ and CS– odorants. Arrow indicates a bout of high-frequency sniffing during the intertrial interval.

them to carry out a lick/no-lick two-odor discrimination task (**Fig. 1a**) for up to 90 min per daily session. Head-fixed rats showed respiration rates that were typical of unrestrained rats in a familiar environment[5], with a mean frequency of 2.37 ± 1.79 Hz (n = 51,619 cycles, four rats, four sessions per rat) and a variable instantaneous frequency of 1–10 Hz (**Fig. 1b**). Because of the continuous distribution of respiration rates observed throughout a session (**Fig. 1b**), we use 'sniffing' to refer to all respiratory activity regardless of frequency[10]. When discriminating familiar odorants, rats showed either no change or slight (~1 Hz) increases in respiration rate around the time of odor discrimination (**Fig. 1c**, **Supplementary Fig. 3** and **Supplementary Results** online). Despite a lack of high-frequency (>4 Hz) sniffing during the discrimination of familiar odorants, task performance in head-fixed rats was highly accurate and qualitatively similar to that reported for freely moving rats (**Supplementary Results**). After the animals reached adequate performance levels (**Supplementary Table 1** online), ORNs were loaded with calcium-sensitive dye[22] and an optical window was installed over the dorsal bulb. Optical signals reflecting ORN input to dorsal glomeruli were then imaged in 4–5 subsequent behavioral sessions. To avoid confounds between sniffing and licking, only data from unrewarded (CS–) trials that did not elicit licking were analyzed.

Spatiotemporal patterns of olfactory input in the awake rat

We began with a basic characterization of spatiotemporal patterns of sensory input to the olfactory bulb imaged from the awake rat. Odorant-evoked optical signals were first subjected to an initial preprocessing and data reduction step (**Supplementary Fig. 4** and **Supplementary Methods** online). Signals appeared as foci with a mean diameter (half-width) of 162 ± 57 μm (mean ± s.d.; range, 61–289 μm; n = 40), consistent with their reflecting ORN input to single glomeruli or to small clusters of adjacent glomeruli. Spatial patterns (that is, 'maps') of ORN input to glomeruli were odorant specific and consistent across daily sessions (**Fig. 2a**), with relative response amplitudes in different glomeruli typically varying by less than 20% across days. Response maps were distributed and fragmented, with a loosely chemotopic clustering of activated glomeruli in dorsomedial and caudolateral domains[22,23]. Movement artifacts were minimal (**Supplementary Video 1** online).

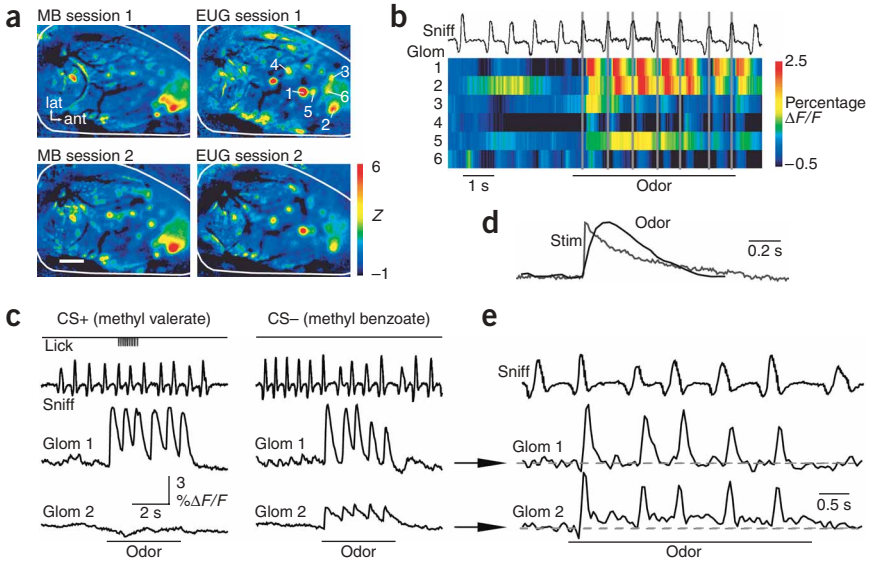

Figure 2 Receptor input to the olfactory bulb imaged in the awake behaving rat. (**a**) 'Sniff-triggered average' maps of responses to two odorants (MB, methyl benzoate; EUG, eugenol) imaged from the same rat on subsequent days. Each map is z-scored and displayed according to the color scale at lower right. Approximate border of imaged region is shown in white. Scale bar, 500 μm. (**b**) Time series of responses of six glomeruli (locations indicated in **a**) to EUG in a single trial. Vertical lines mark the peak of each inspiration during odorant presentation. Time bin, 40 ms. Most glomeruli (but not all; see glom 5) responded shortly after inspiration. Latency differences between glomeruli (for example, gloms 1 and 2) are recapitulated with each sniff. Glomerulus 6 responded to inspirations independent of odorant presentation. (**c**) Lickometer signal (top), sniff records and presynaptic calcium signals imaged from two glomeruli during a two-odor discrimination task (different animal from that in **a**). Optical signals are unfiltered. Sniff signals are low-pass filtered at 12.5 Hz. (**d**) Odorant-evoked calcium signal after one sniff in an awake rat ('odor') and nerve shock–evoked signal in an anesthetized rat ('stim'). Traces are scaled to the same amplitude and aligned to the start of each response. (**e**) Temporally deconvolved calcium signals (same CS– trial and glomeruli as in **c**) reflecting estimated action potential firing patterns in ORNs converging onto each glomerulus.

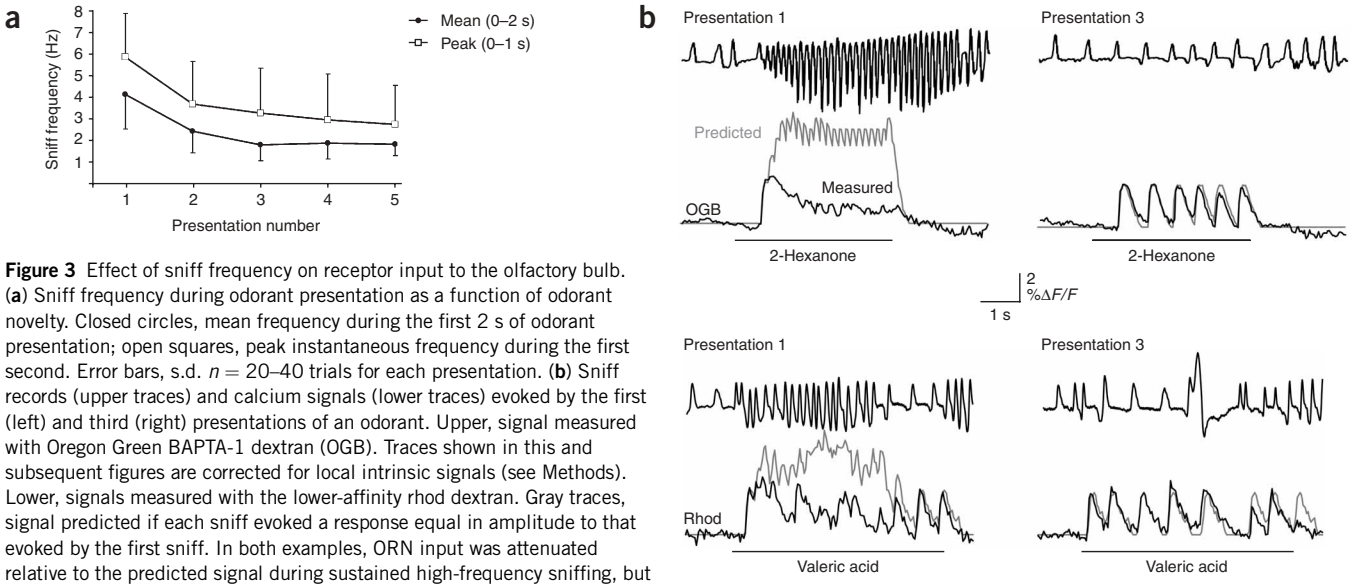

Figure 3 Effect of sniff frequency on receptor input to the olfactory bulb. (**a**) Sniff frequency during odorant presentation as a function of odorant novelty. Closed circles, mean frequency during the first 2 s of odorant presentation; open squares, peak instantaneous frequency during the first second. Error bars, s.d. $n = 20$–40 trials for each presentation. (**b**) Sniff records (upper traces) and calcium signals (lower traces) evoked by the first (left) and third (right) presentations of an odorant. Upper, signal measured with Oregon Green BAPTA-1 dextran (OGB). Traces shown in this and subsequent figures are corrected for local intrinsic signals (see Methods). Lower, signals measured with the lower-affinity rhod dextran. Gray traces, signal predicted if each sniff evoked a response equal in amplitude to that evoked by the first sniff. In both examples, ORN input was attenuated relative to the predicted signal during sustained high-frequency sniffing, but not during low-frequency sniffing. The example in the lower panel shows that responses recovered later in the trial, as sniff frequency decreased.

As in anesthetized mice[14], we saw diverse temporal patterns of ORN input to glomeruli in awake rats (**Fig. 2b**). At low sniff frequencies (1–3 Hz), the dominant pattern consisted of calcium signals that were phasic and tightly coupled to the sniff cycle (**Fig. 2b**,**c**), with a latency from start of inhalation to 10% of response maximum (t_{10}) of 110 ± 28 ms and a time to peak (t_{10} to peak signal) of 167 ± 78 ms ($n = 36$ trials, ten glomeruli, one animal imaged at 100 Hz; similar latencies were obtained from five additional rats imaged at 25 Hz). Decay times varied (**Fig. 2c**), but were often similar to the decay times seen after single olfactory nerve shocks (**Fig. 2d**), suggesting that ORN firing ceases rapidly after inhalation.

To better estimate the temporal dynamics of ORN action-potential firing across the population of ORNs innervating a glomerulus, we performed temporal deconvolution of sniff-evoked calcium signals[24] using the decay constant measured after a single olfactory nerve shock in urethane-anesthetized rats (**Fig. 2d** and **Supplementary Methods**). Deconvolved calcium signals appeared as brief peaks that returned rapidly to baseline (width at half-maximum, 145 ± 21 ms; $n = 83$ glomeruli, five sessions, one animal; **Fig. 2e**). Although these estimates are subject to a small degree of error due to factors such as dye saturation and presynaptic modulation of calcium influx[25], they nonetheless suggest that each sniff drives rapid activation of ORN input to a glomerulus, and that ORN firing decreases rapidly after each initial burst. Thus, at sniff frequencies below 3 Hz, ORN inputs to the olfactory bulb occur mainly as brief bursts after each inspiration.

Effect of high-frequency sniffing on odorant response maps

Rodents increase sniff frequency under many circumstances[6,7,9]. In our protocol, presentation of a novel odorant (presented as CS–) elicited a bout of investigative sniffing at 4–6 Hz (duration of >4-Hz sniffing bout, 2.06 ± 1.1 s, $n = 25$ trials). Sniff frequency decreased as a function of exposure number (one-way ANOVA, $F_{4,164} = 45.2$, $P < 10^{-23}$), habituating in 1–2 trials (**Fig. 3a**). We could thus compare ORN inputs evoked by high- and low-frequency sniffing of the same odorant, separated in time by only a few trials (typically 30–90 s) (**Fig. 3b**).

Sniffing is hypothesized to alter patterns of ORN activity to optimize odor detection or discrimination[7,13,26]. To address this hypothesis, we compared response maps evoked by low-frequency (<2.5 Hz) and high-frequency (>4 Hz) sniffing of the same odorants (**Fig. 4a**). For quantitative comparison, maps were made from the peak response amplitudes evoked during the first second of sniffing at either frequency. Maps were compared using the mean absolute difference in response (MAD) between all glomeruli in each map pair (**Fig. 4b**). The MAD values between high- and low-frequency sniffing response maps (median = 0.46, $n = 20$ map pairs) were not statistically different from those between response maps made from repeat trials of the same odorant (median = 0.46, $n = 18$ map pairs, $P = 0.804$, two-sided Wilcoxon rank sum test). Thus, high-frequency sniffing did not significantly alter patterns of ORN activation when a single odorant was sampled in isolation.

High-frequency sniffing may also enhance ORN response by increasing odorant flow over the olfactory epithelium[5,7]. To test this hypothesis, we compared peak response amplitudes of individual glomeruli that were evoked by low- and high-frequency sniffing (taken from the same data as above). As expected from the similarity in response maps, response amplitudes were strongly correlated ($r = 0.81$, $n = 532$ glomerulus-odorant pairs, five animals; **Fig. 4c**). However, high-frequency sniffing slightly increased the amplitude of responses in the lower or middle third of the dynamic range of a glomerulus (lower third: $P < 0.001$, $n = 98$; middle third: $P < 0.0001$, $n = 59$; two-sided paired t-test), but did not do so for those in the upper third ($P = 0.54$, $n = 83$) (**Fig. 4d**). Although statistically significant, the absolute increase in response amplitude for high- versus low-frequency sniffing was small, covering 0.10 ± 0.03 (mean ± s.e.m.) of the dynamic range for low-amplitude responses and 0.13 ± 0.03 for mid-level responses. Thus, increasing sniff frequency only modestly enhanced weak ORN inputs to glomeruli.

Sustained high-frequency sniffing attenuates ORN inputs

It has been proposed that each sniff generates a perceptually complete 'snapshot' of the odor environment[8,10]; high-frequency sniffing thus allows more snapshots to be acquired per unit time. This hypothesis predicts that, during high-frequency sniffing, phasic inputs to glomeruli should be repeated with each sniff, or that inputs should be tonically

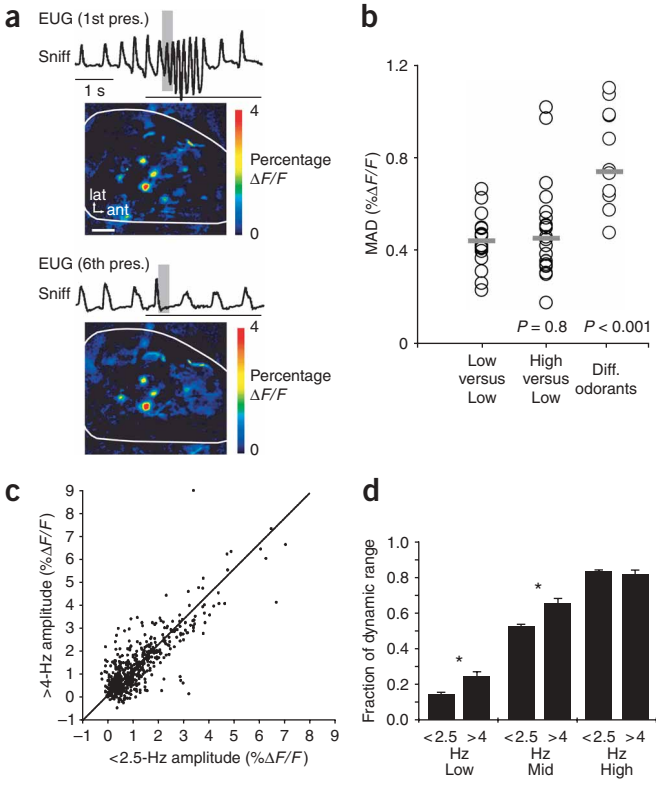

Figure 4 Minor effect at the onset of high-frequency sniffing on odorant response maps. (**a**) Response maps evoked by high (>4 Hz) and low (<2.5 Hz) frequency sniffing of EUG. Sniff traces for each trial are above each map. Gray box indicates time-averaged window used to construct maps. (**b**) Quantitative comparison of response maps during low- and high-frequency sniffing. Maps were based on the maximal response in the first second after odorant presentation. Higher MAD values indicate less similarity. Open circles, MAD value for each comparison; gray bars, the median value. 'Low versus Low' compares repeat trials of the same odorant during low-frequency sniffing; 'High versus Low' compares same-odorant trials at high and low sniff frequencies; 'Diff. odorants' compares maps for different odorants tested in the same session. *P*-values show the results of comparing each set of MAD values with those from repeat trials (Wilcoxon rank sum). (**c**) Peak response amplitudes during the first second of odorant presentation evoked in all glomeruli by low- and high-frequency sniffing. Black line shows the diagonal. (**d**) Effect of sniff frequency on response amplitudes (mean ± s.e.m.) after normalizing responses to the dynamic range of each glomerulus. Data are taken from the subset of glomeruli in **c** that responded with a high signal-to-noise ratio to any odorant (see **Supplementary Methods**). Dynamic range was defined from zero to the maximal response evoked by any odorant in a session. Response pairs are grouped into 'low', 'mid' and 'high' thirds of the range. *Significant difference (paired *t*-test; $P < 0.001$) between low- and high-frequency sniffing.

maintained at high levels. Instead, we found the opposite: during high-frequency sniffing, ORN inputs were not driven by each sniff, but instead appeared mainly as tonic signals (**Fig. 3b**). Rather than being maintained at high levels, the tonic signals became attenuated (**Fig. 5a** and **Supplementary Fig. 5** online). After 3 s of sustained high-frequency sniffing, the amplitude of the tonic calcium signal was 0.50 ± 0.06 (mean ± s.e.m.; $n = 80$ responses) relative to that at the onset of sniffing. In contrast, tonic calcium signals evoked by trains of olfactory nerve shocks designed to simulate 5-Hz sniffing for 1 s showed sustained amplitude increases (**Supplementary Fig. 6** online).

Phasic responses driven by each sniff were nearly eliminated at sniff frequencies >4 Hz (**Fig. 5b**; response amplitude after 2 s of odor stimulation, 0.18 ± 0.01 of initial response; mean ± s.e.m., $n = 396$). Identical results were obtained with the lower-affinity dye rhod dextran ($K_d = 1.65$ μM; **Fig. 3b** and **Supplementary Fig. 5**). The loss of phasic responses was not due to an inability of the calcium signal to report phasic inputs at these frequencies, as glomeruli easily followed trains of nerve shocks that were delivered at 5 Hz (**Supplementary Fig. 6**). ORN inputs showed only modest attenuation during low-frequency sniffing of the same odorants (response amplitude after 2 s of odor stimulation, 0.60 ± 0.02 of initial response; mean ± s.e.m., $n = 492$; **Fig. 5c**). These response amplitudes could be maintained for as long as 2 min with continuous odorant stimulation (data not shown). We observed similar effects of sniff frequency even for weakly activated glomeruli,

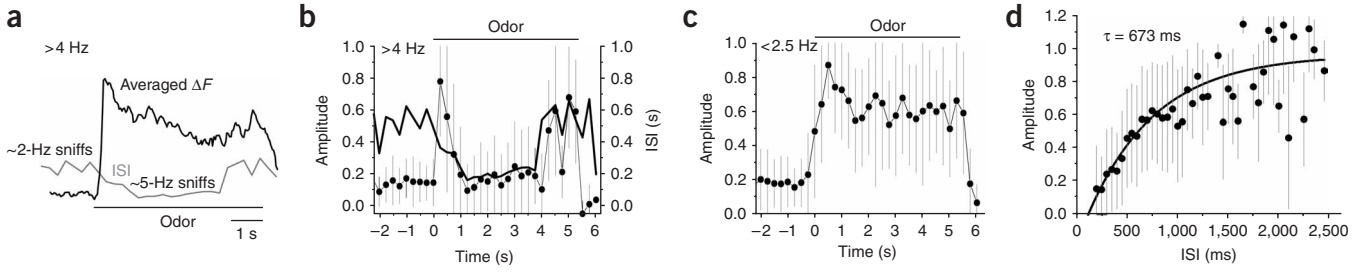

Figure 5 High-frequency sniffing attenuates ORN inputs to the olfactory bulb. (**a**) Averaged, normalized response traces from high-frequency sniffing trials, emphasizing the tonic component of the response. Trace is the average of 80 individual traces (one trace per glomerulus per odorant; four animals). Traces were aligned and normalized to the maximum amplitude observed after the first sniff after stimulus onset. Gray line shows the mean ISI for these trials (also plotted in **b**). Sniffing frequency changed from ~2 Hz to ~5 Hz at odorant onset and then typically slowed later in the trial. The response also began to recover as sniff frequency slowed. (**b**) Response amplitudes (filled circles) evoked by each sniff, compiled from the same trials as in **a**. These data reflect the phasic component of each sniff-evoked response (see **Supplementary Methods**). Amplitudes were normalized to the maximum response observed in the first 2 s of odorant presentation (typically the first sniff) and placed into 250-ms time bins according to the time of the preceding sniff (~100 total sniffs per bin). Error bars, s.d. Solid black line, mean ISI for the trials (s.d.: 153 ± 89 ms). Phasic response amplitudes recovered as sniff frequency decreased later in the trial. (**c**) Sniff-evoked response amplitudes for low-frequency sniffing trials displayed as in **b**. Glomeruli and odorants were the same as in **b**. $N = 165$ trials (unique glomerulus-odorant pairs). (**d**) Sniff-evoked response amplitude versus ISI. Data are taken from all non-novel odorant CS– trials. Points indicate mean ± s.d. of the peak calcium signal evoked by each sniff. Data are compiled from 7,753 sniff-evoked responses. Solid line, maximum-likelihood fit of single-exponential function to data ($\tau = 673$ ms; **Supplementary Methods**).

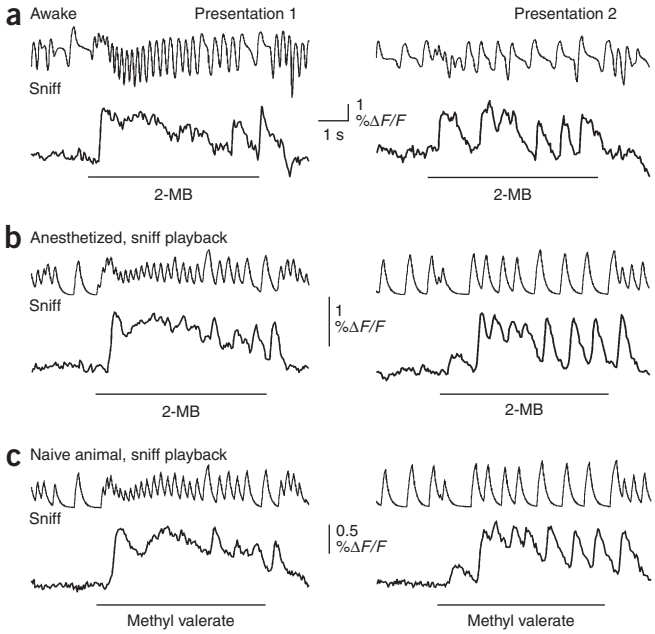

Figure 6 Frequency-dependent attenuation of ORN inputs results from low-level processes. (**a**) Sniff records and presynaptic calcium signals evoked by the first (left) and second (right) presentations of 2-methylbutyraldehyde (2-MB). The first presentation elicited a bout of high-frequency sniffing and response attenuation. Responses to each sniff recovered as sniffing slowed later in the trial. Sniffs occurred at lower frequencies for the second presentation, with no response attenuation. (**b**) Sniff playback experiment. The animal from **a** was anesthetized and the sniffing recorded in **a** was used to drive an artificial sniff device (see Methods). Odorant, concentration and glomerulus is the same as in **a**. Traces are averages of seven trials. Sniff records show pressure measured via the intranasal cannula, as in **a**. (**c**) Responses evoked by the same sniff patterns in a different, naive animal and using a different odorant. Traces are averages of four trials. Response patterns in **b** and **c** are similar to those seen in the awake rat, showing sniff frequency–dependent response attenuation and recovery (left) and little attenuation at low sniff frequencies (right).

though we did not analyze these quantitatively because of signal-to-noise limitations.

Although we used novel odorants to reliably elicit high-frequency sniffing, several lines of evidence indicated that attenuation of ORN inputs was a function of sniff frequency, not odorant novelty. First, phasic sniff-evoked response amplitudes recovered during novel odorant trials as sniff frequency decreased later in the trial (**Fig. 3b**). On average, sniff-evoked response amplitudes closely paralleled the inter-sniff interval (ISI) during high-frequency sniffing trials (**Fig. 5b**). Second, in data compiled from all non-novel odorant trials, there was a strong relationship between ISI and response amplitude (**Fig. 5d**). Mean response amplitudes for each 50-ms ISI time bin were well fit by a single-order exponential decay function with a time constant of 673 ms (modified maximum-likelihood fit, $n = 7{,}753$ responses, 4 animals, 16 sessions, $r^2 = 0.77$; see **Supplementary Methods**). Thus, instantaneous sniff frequency is a strong determinant of the magnitude of ORN input to a glomerulus. Third, attenuation of both phasic and tonic inputs also occurred for familiar odorants when rats increased sniff frequency either in response to a novel auditory stimulus or spontaneously (**Supplementary Fig. 7** online).

If frequency-dependent attenuation of ORN inputs depends on low-level processes such as receptor adaptation, it should persist independent of behavioral state. To test this, we recorded responses to initial and subsequent presentations of novel odors in an awake rat (**Fig. 6a**). The rat was later anesthetized, a double tracheotomy performed, and an artificial sniff protocol used to draw odorant into the nasal cavity[14]. Sniffing patterns recorded from the awake animal were then 'played back' in the anesthetized animal using the same odorants. To control for possible order effects, low-frequency sniffing trials were imaged before high-frequency trials, which was opposite from their order in the awake state. Responses imaged from the same glomeruli were qualitatively similar to awake responses (**Fig. 6b**), showing a loss of sniff-driven phasic responses and an attenuation of tonic responses, with response recovery as sniff frequency decreased later in the trial (**Fig. 6b**). We performed the playback experiment in a second, naive rat using a different odorant with similar results (**Fig. 6c**). These results suggest that attenuation of ORN inputs is a general phenomenon mediated by low-level processes and does not depend on centrifugal modulation by behavioral state.

Adaptive filtering of ORN inputs

We hypothesized that attenuation of ORN inputs at high sniff frequencies could facilitate odor detection in a changing odor landscape by reducing ORN responsiveness to background odorants. To test this idea, we induced high-frequency sniffing of a novel odorant; this odorant then served as the 'background' odorant for the duration of the trial. In the midst of the high-frequency sniff bout, we introduced a second odorant (the 'test' odorant) into this background stream. In one such experiment, for example (**Fig. 7a**), we used 2-butanone as the background and ethyl butyrate as the test odorant. When presented alone, the two odorants evoked input to partially overlapping sets of glomeruli (**Fig. 7a**,**b**). In the background/test experiment, 2-butanone elicited high-frequency sniffing, along with an initial calcium signal that was followed by attenuation (**Fig. 7a**). Introduction of the test odorant (ethyl butyrate) during the high-frequency sniff bout did not evoke a response in those glomeruli that were already activated by 2-butanone, but still evoked strong responses in other glomeruli (**Fig. 7a**). This effect was not a result of mixture interactions, as the two odorants evoked strong input to both glomeruli when they were presented together during low-frequency sniffing (data not shown, but see maps in **Fig. 7b**). Thus, although high-frequency sniffing attenuates input from responsive ORNs, it does not affect the ability of other ORNs to respond to other odorants encountered later in the sniff bout.

Glomerulus-specific, sniff-frequency–dependent attenuation of ORNs systematically altered odor representations in the olfactory bulb. In our background/test experiment, the response map that was evoked by the test odorant presented during high-frequency sniffing of the background appeared to be similar to the difference between the maps evoked by each odorant alone (**Fig. 7b**). In contrast, the response map that was evoked by the same stimuli presented during low-frequency sniffing was similar to the maximum of the two single-odorant maps (**Fig. 7b**). Thus, the same stimulus could be represented by different response maps depending on sniff frequency.

We confirmed this observation statistically by comparing maps from ten such experiments (three animals) using the MAD between all glomeruli in each map pair (**Fig. 7c**). First, maps evoked by the test stimulus presented during high-frequency sniffing of the background (presented as in **Fig. 7a**) differed from those evoked when the test stimulus was presented during low-frequency sniffing of the background ($n = 6$), or when the test and background odorants were presented together during low-frequency sniffing ($n = 4$) (**Fig. 7c**; $P < 0.001$, two-sided Wilcoxon rank sum). Second, maps differed

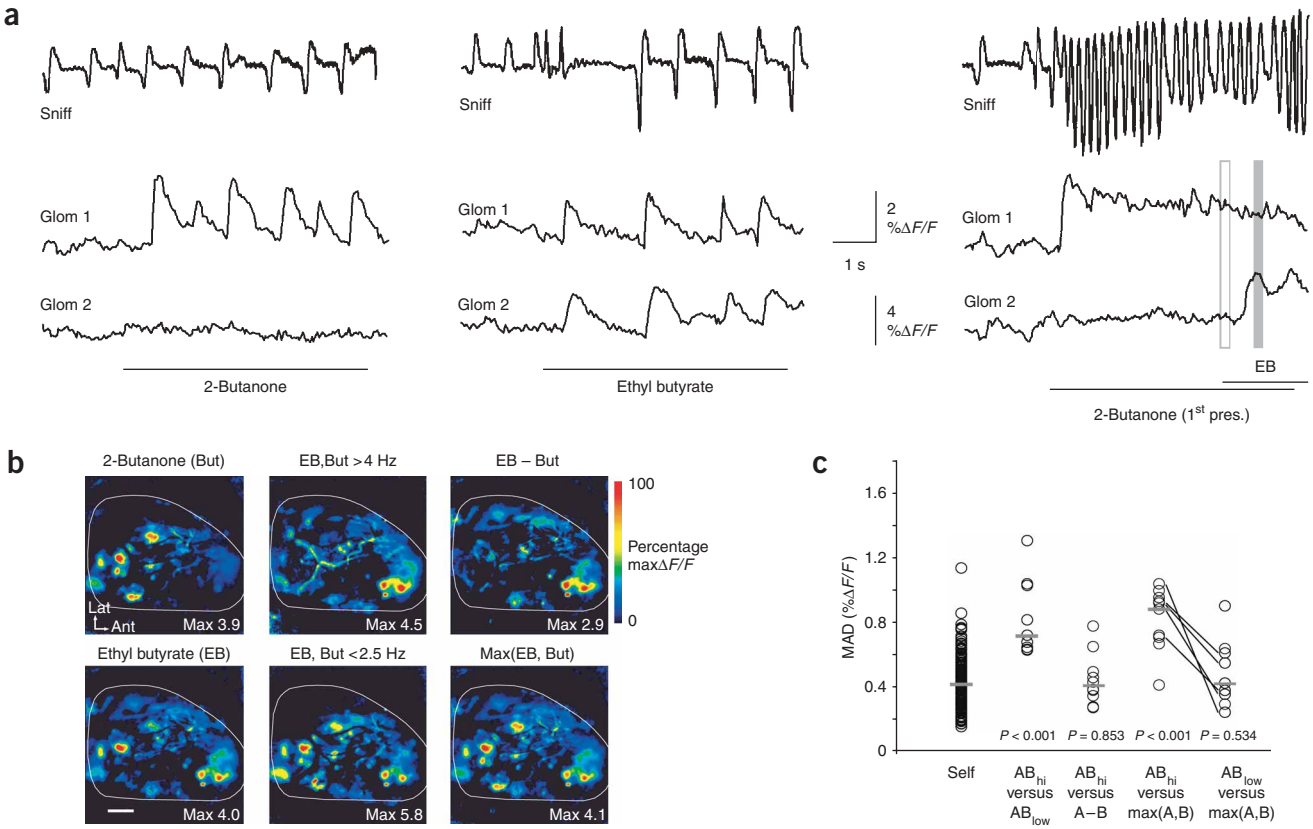

Figure 7 Adaptive filtering of ORN inputs controlled by sniff frequency. (**a**) The background/test odorant experiment. Traces show sniff records (top) and optical signals from two glomeruli (lower traces). Glomerulus 1 responded to 2-butanone and ethyl butyrate; glomerulus 2 responded only to ethyl butyrate (two left columns). High-frequency sniffing of 2-butanone (right column) caused response attenuation in glomerulus 1, with no further response when ethyl butyrate (EB) was presented later in the trial. Glomerulus 2 responded strongly to EB. (**b**) Response maps from the experiment in **a**. Left, responses to individual odorants (average of responses to first sniff in each of four trials). Top middle, response to EB presented during high-frequency sniffing of 2-butanone (time windows used for maps are shown in **a**). Bottom middle, response to the two odorants presented as a binary mixture during low-frequency sniffing (first sniff, one trial). Upper right, subtraction of the background odorant map from the test odorant map. Lower right, map of the maximal combination of the background and test maps. Maximum %$\Delta F/F$ values ('Max') are shown for each map. Scale bar, 500 μm. (**c**) Comparison of response maps in the background/test odorant experiments. Higher MAD values indicate less similarity. Open circles show the MAD for each comparison; gray bars, the median value. Which maps were compared is indicated below each column of data. 'A' and 'B' represent the test and background odorant, respectively ($n = 10$ experiments). Self, comparison between repeated trials of the same odorant ($n = 145$). AB_{hi}, response to A presented during high-frequency sniffing of B ($n = 10$). AB_{low}, response to A either presented during low-frequency sniffing of B ($n = 6$) or presented along with B during low-frequency sniffing ($n = 4$). A–B, B response map subtracted from A map. Max(A,B), maximum of A and B maps. P values show the results of comparing each set of MAD values with those from repeat trials (Wilcoxon rank sum). Solid lines connect MAD values in which A was presented during both high- and low-frequency sniffing of B in the same experiment ($n = 5$); responses became more similar to maximal combination maps as sniff frequency slowed.

systematically depending on sniff frequency. Test/background response maps during high-frequency sniffing were similar to maps constructed by subtracting the background from the test map ($P = 0.85$; Wilcoxon rank sum). In contrast, test/background response maps during low-frequency sniffing were similar to maps made by taking the maximum of the background and test maps ($P = 0.53$; Wilcoxon rank sum). This latter result was true when the test odorant was presented after the onset of the background odorant ($n = 6$) or when the two odorants were presented together ($n = 4$). Thus, high-frequency sniffing alters odor coding by effectively subtracting glomeruli sensitive to background odorants from the representations of odorants encountered later.

DISCUSSION

Many studies have characterized odor representations in the olfactory bulb of anesthetized rodents[14,22,23,27]. Here, imaging ORN input to the bulb in awake rats revealed previously unknown features of odor representations and their relationship to sampling behavior ('sniffing'). Sniffing is fundamental in shaping how odor information is conveyed from the periphery to the olfactory bulb. At the low sniff rates seen in the resting animal, each inspiration evokes a transient (100–200 ms) burst of ORN input, with only moderate reduction in amplitude over repeated sniffs. At the higher sniff rates typical of active exploration or investigation of a novel stimulus, however, transient inputs locked to inspiration largely disappear and are replaced by tonic, attenuated inputs. This attenuation is specific to activated glomeruli, leaving other glomeruli still able to respond to subsequently encountered odorants. This organization constitutes an adaptive filter for odor information that is implemented at the level of the primary receptor neurons and is under behavioral control through alteration of sniff frequency.

Odor discrimination performance in restrained animals has not previously been characterized. Performance accuracy, response times, the ability to learn new odor associations with relative ease and the ability to detect and investigate novel odorants all suggest that

odor-guided behavior is not seriously compromised in head-fixed animals. To our surprise, although head-fixed rats showed respiration rates that were typical of calm, unrestrained rats in a familiar environment[4,5], they showed little or no increase in sniff frequency when performing odor discriminations. In contrast, unrestrained rats performing a nose-poke into an odor port increase sniff rates to 4–10 Hz around the time of odor sampling[7,8,11,28]. One explanation for these differences is that high-frequency sniffing may primarily be driven by expectation or movement toward an odor source, and may not be necessary, or even important, for discriminating one odorant from another. This hypothesis is consistent with the finding, discussed in more detail below, that sniff frequency has little impact on spatial odor representations in the olfactory bulb when that odorant is sampled in isolation.

Switching between passive respiration and active sniffing involves substantial changes to the airflow through the nasal cavity and over the olfactory epithelium[7,29]. Such changes are hypothesized to shape odor coding by altering odorant sorption on the epithelium and the resulting spatiotemporal patterns of ORN activity[7,13,26]. However, we found that sampling the same odorant at high or low sniff rates yielded initial response maps (taken during the first second of odorant sampling) that were similar. High-frequency sniffing only slightly increased ORN inputs to those glomeruli that were weakly activated or nonresponsive at low sniff rates, with no change in the inputs to other glomeruli. These increases covered only ~10% of the estimated dynamic range of the glomerulus. Thus, although high-frequency sniffing may slightly enhance odor detection ability, it seems to have little impact on the overall spatial representation of odors in the olfactory bulb.

In contrast, sniff frequency substantially affected the temporal structure and magnitude of ORN inputs during sustained odorant sampling. Within 1 s of sampling at high frequencies (>4 Hz), transient inputs that were phase-locked to each inspiration nearly disappeared. The loss of sniff-driven inputs was not a result of dye saturation or of an inability to follow inputs at this frequency. Tonic levels of calcium signals were also attenuated during high-frequency sniffing, indicating that, in addition to a loss of respiration-linked temporal patterning, overall levels of ORN input were strongly reduced during high-frequency sniffing.

The primary mechanism underlying sniff frequency–dependent attenuation of ORN inputs may be receptor adaptation. Higher sniff frequencies allow less time for ORNs to recover from adaptation between inspirations, and they probably include a tonic component in which odorant is continuously entering the nasal cavity[7,8]. Recordings from rat ORNs *in vivo* show that neurons respond to odorant pulses with brief (<100 ms) action potential bursts[30], and receptor currents in isolated mouse ORNs show ~80% adaptation in 2 s[31], a time course similar to the speed with which ORN inputs attenuated. In contrast, we observed little attenuation at low sniff frequencies (1–2 Hz), which is consistent with the fact that olfactory bulb mitral cells show little adaptation in anesthetized rats breathing at similar frequencies[32]. A secondary mechanism that may contribute to the attenuation of ORN inputs is the suppression of calcium influx into ORN presynaptic terminals that is mediated by intraglomerular feedback inhibition[25,33]. In olfactory bulb slices, this inhibition reaches peak suppression levels of ~40% at interstimulus intervals of 100–200 ms and decays with a time constant of ~500 ms[25], which is consistent with the frequency dependence of sniff-driven responses we observed.

The different temporal structure of ORN inputs to the olfactory bulb during low- and high-frequency sniffing has important consequences for information processing in the bulb and for odor coding strategies. ORN inputs driven by sniffing have been hypothesized to shape the strength of inhibition within and between glomeruli[19] and to facilitate synchronous firing of mitral/tufted (M/T) cells as well as granule cell interneurons[17,18]. The phase of M/T firing relative to the respiratory cycle is also hypothesized to encode odor information[20,21,34,35]. Yet, we found that although respiratory patterning of ORN input was strong and reliable at low sniff frequencies, patterning was weaker or lost entirely at frequencies typical of active odor sampling. Thus, phenomena observed in anesthetized animals[21] or in olfactory bulb slices receiving patterned stimulation[17–19] may be much less prominent in awake, actively sniffing animals. M/T cell recordings from awake animals show that M/T firing decouples from respiration at sniff frequencies above 4 Hz[11,36,37]. Decoupling was originally thought to reflect increased modulation by centrifugal inputs[11,37], but a breakdown in respiratory patterning at the level of ORN inputs seems a more likely explanation. Indeed, reproducing high-frequency sniff patterns in anesthetized animals yielded attenuation and loss of patterning that was markedly similar to that seen in awake rats. Centrifugal inputs to the bulb may still carry information about respiratory cycle during high-frequency sniffing, and thus patterned receptor inputs are not necessary for patterned M/T cell firing or for a respiration phase-based code[34,35]. However, given the evidence that M/T dynamics are more strongly shaped by the dynamics of ORN inputs than by respiration-driven centrifugal signals[15], it seems likely that the switch in ORN activity from a phasic, respiration-driven pattern to a predominately tonic one could change the nature of information processing and coding in the olfactory bulb.

Because mice and rats can perform simple odor discriminations after a single sniff, it has been proposed that each sniff provides a unitary, 'fully refined' representation of the olfactory environment[8,10]. In contrast, our data suggest that these representations are highly plastic. The same odorant, especially when presented against a background odorant, can evoke different representations depending on how the odorant is sampled. This process is very likely to occur during natural odor-guided behaviors, in which both sniffing behavior and the odor environment are complex and temporally dynamic. Paradoxically, high-frequency sniffing may actually increase the necessity for rapid odor discrimination; attenuation of ORN inputs after the first one or two sniffs of an odorant may increase the detection threshold or otherwise change the odor representation such that the discrimination ability is degraded after the initial response.

What, then, is the advantage of sniffing at a high frequency? Because rapid sniffing effectively subtracts ORN inputs that are activated by background odorants from odor representations in the olfactory bulb, we propose that one function of rapid sniffing is to allow the animal to suppress signals from background odor sources, and thus to detect newly encountered (and thus potentially more important) odorants more clearly. Although we used novel odorants presented against a 'clean' background to induce high-frequency sniffing in our protocol, frequency-dependent attenuation occurred independent of odorant novelty, suppressing inputs from any odorants present when a sniff bout begins. Thus, adaptive filtering of inputs under the control of sniff frequency is a general phenomenon that is optimally suited for scanning the environment for changes in odor composition or concentration[38], and it may explain why high-frequency sniffing is induced by any novel stimulus or during exploratory behavior[6,9]. Because it involves higher sampling rates, active sniffing allows for a more rapid detection of stimulus changes. The speed of adaptive filtering also allows for rapid behavioral control of the mode of odor detection: attenuation at high frequencies occurs in less than 1 s, and recovers in less than 1 s after sniff frequency slows. Thus, an animal can rapidly switch from detecting changes in the odor landscape during

high-frequency sniffing to surveying the odor scene *in toto*, depending on task demands (**Supplementary Fig. 8** online). Humans can modulate sniff duration as well as frequency during active odor sampling[3,12]; in this case, prolonged odorant inhalation may also attenuate receptor inputs, enhancing the ability to detect changing olfactory stimuli in a single long sniff.

Sniff frequency–dependent filtering of sensory input to the olfactory bulb provides a mechanism by which behavioral state can modulate how sensory information is encoded and processed with little contribution from centrifugal projections or other network phenomena. Modulation of sensory coding as a function of experience or behavioral state is well established, but it generally results from higher-order processes. Examples include centrifugal modulation of M/T cell responses in the olfactory bulb[11,36], the slow adaptation to background odorants mediated by synaptic depression in piriform cortex neurons[39] and modulation of auditory cortex neuron responses during vocal behavior[40]. Adaptive filtering of ORN inputs is a unique example of a low-order, 'bottom-up' process for modulating sensory codes. Other modalities that rely on rhythmic sampling at behaviorally controlled frequencies (such as licking and whisking) may use similar strategies. Finally, given that sniffing behavior substantially alters spatial and temporal patterns of ORN activity and that these patterns are widely thought to underlie odor quality perception[41–43], we predict that odor perception depends not only on stimulus identity, but also on the way the stimulus is sampled.

METHODS

All procedures were approved by the Boston University Institutional Animal Care and Use Committee and were in accordance with guidelines established by the US National Institutes of Health. All statistics report mean ± s.d. unless otherwise noted. Detailed methods can be found in the **Supplementary Methods** online.

Surgical procedures. Adult female Long-Evans rats ($n = 7$; mean body weight at imaging, 242 g) were used. In an initial procedure, a guide cannula was implanted in the dorsal recess of one naris for intranasal pressure measurements, and a head bolt implanted on the skull for restraint[44]. After behavioral training and 3–4 d before the first imaging session (see below), ORNs in both nares were loaded with dextran-conjugated calcium-sensitive dye[22]. Oregon Green BAPTA-1 488 dextran (10 kDa) was used in six of seven rats; 'high-affinity' rhod dextran (10 kDa) was used in one rat. One day before the first imaging session, the bone overlying each olfactory bulb was thinned and a chronic optical window installed. Optical data were obtained from each animal over four or five consecutive daily sessions.

Behavioral training. Animals were trained to accept head fixation and to perform odor discriminations using water restriction for motivation. All training and imaging was performed in a custom chamber installed under the imaging apparatus. One to two weeks after the initial surgery, rats were water-deprived and handled daily. Rats were habituated to head restraint by gradually increasing the duration of restraint and by providing water rewards through a lick spout. When the interval between water rewards reached approximately 10 s, rats were made to discriminate one rewarded odorant (CS+) from multiple unrewarded odorants (CS–) in a lick/no-lick discrimination protocol (for details see **Supplementary Methods**). The intertrial interval varied randomly between 15–24 s. Imaging began after rats reached adequate performance levels on the task (see **Supplementary Table 1**). Odorant delivery, sniffing measurements and monitoring of performance was achieved through custom software written in LabVIEW (National Instruments).

Olfactometry. Odorants were simple, monomolecular hydrocarbon compounds and included ketones, aldehydes, organic acids, esters and benzene derivatives. All odorants were obtained from Sigma-Aldrich and were of the highest available purity. Odorants were diluted from saturated vapor of pure liquid odorant and presented via a multichannel, computer-controlled flow-dilution olfactometer[14]. Dilutions ranged from 0.5–5% of saturated vapor (typical dilution was 1%). For 'sniff playback' experiments in anesthetized animals, an artificial sniff protocol was used[22], but with the intranasal vacuum solenoid controlled by a thresholded, digital representation of previously recorded sniff records. Sniff flow rates were 150–250 ml min^{-1}.

Optical recordings. Calcium signals were imaged in head-fixed rats using a custom-built imaging apparatus with Olympus epifluorescence optics (BX51). The olfactory bulb was illuminated with full light from a 150-W xenon arc lamp (Opti-Quip) and visualized with the following filter set: HQ480/40 (excitation), Q505LP (dichroic) and HQ535/50 (emission). A region of the dorsal bulb spanning 2.8 ± 0.2 mm in the rostrocaudal dimension and 1.5 ± 0.1 mm in the mediolateral dimension was imaged using a 4×, 0.28-NA objective (Olympus). Images were acquired with a 256 × 256 pixel CCD camera (NeuroCCD; SM-256, RedShirtImaging LLC) at 25- or 100-Hz frame rates. The camera resolution was 13.1 μm per pixel. The anterior and posterior edges of the imaged region were at approximately 9.9 and 7.1 mm anterior to bregma, respectively, and the medial and lateral edges at 0.3 and 1.8 mm lateral to midline, respectively.

Data analysis. Optical signals were synchronized with recordings of sniffing, behavior (licking) and odor delivery times and saved using Neuroplex software (RedShirt Imaging). All subsequent analyses were performed with custom software written in Matlab (Mathworks). Optical signals were first corrected for potential movement artifacts and spatially high-pass filtered to reduce global fluorescence changes due largely to intrinsic signals, then regions of interest (ROIs) representing responsive glomeruli were chosen manually and their optical signals extracted for further analysis.

Signals from each ROI were corrected for localized intrinsic signals associated with blood vessels (**Fig. 3b** and **Supplementary Fig. 5**; see **Supplementary Methods**). For map comparisons (**Fig. 4b** and **Fig. 7c**), MAD between maps was calculated as $\langle |\Delta F_x / F_x - \Delta F_y / F_y| \rangle$, where x and y indicate different odorant and/or sniffing conditions for the same ROI[27,45]. To construct difference maps (**Fig. 7**), negative response amplitudes (reflecting noise) were clipped at zero before subtraction. For the additive maps, maxima were used rather than the linear sum because of the hypoadditivity of response amplitude in glomeruli that are strongly activated by both odorants[33,46]. Response traces that predicted whether no attenuation occurred (**Fig. 3b**) were generated by choosing a 'typical' response evoked by a single sniff (taken at low sniff frequencies from the same glomerulus); then, for each trial, generating a train of impulses that corresponded to the time of each sniff during odorant presentation; and finally convolving the sniff-evoked signal with the impulse train. Sniff-evoked response amplitudes (**Fig. 5b–d**) were measured automatically from glomerulus-odorant pairs with the highest signal-to-noise ratios (see **Supplementary Methods**). Response maps shown in figures were normalized to their own maximum (defined as mean of the brightest 100 pixels), clipped as indicated and smoothed with a 5 × 5 pixel Gaussian kernel.

Note: Supplementary information is available on the Nature Neuroscience website.

ACKNOWLEDGMENTS

The authors thank D. Katz, A. Fontanini and H. Eichenbaum for help with the restrained preparation and the behavioral paradigm; R. Carey, A. Zaharia and A. Milutinovic for help with data analysis; and M. Shipley, J. McGann and N. Pírez for comments. This work was supported by the US National Institutes of Health and Boston University.

AUTHOR CONTRIBUTIONS

J.V.V., D.W.W. and M.W. contributed to all aspects of the paper, including experimental design, animal training, data collection and analysis. T.I.N. and J.A.W. helped to develop data analysis methods and custom analysis code. All authors contributed to discussing the implications of the results and to preparing the manuscript.

COMPETING INTERESTS STATEMENT

The authors declare no competing financial interests.

Published online at http://www.nature.com/natureneuroscience
Reprints and permissions information is available online at http://npg.nature.com/reprintsandpermissions

1. Reid, R.C. & Alonso, J.M. The processing and encoding of information in the visual cortex. *Curr. Opin. Neurobiol.* **6**, 475–480 (1996).
2. Wilson, R.I. & Mainen, Z.F. Early events in olfactory processing. *Annu. Rev. Neurosci.* **29**, 163–201 (2006).
3. Mainland, J. & Sobel, N. The sniff is part of the olfactory percept. *Chem. Senses* **31**, 181–196 (2006).
4. Macrides, F. Temporal relationships between hippocampal slow waves and exploratory sniffing in hamsters. *Behav. Biol.* **14**, 295–308 (1975).
5. Walker, J.K.L., Lawson, B.L. & Jennings, D.B. Breath timing, volume and drive to breathe in conscious rats: comparative aspects. *Respir. Physiol.* **107**, 241–250 (1997).
6. Welker, W.I. Analysis of sniffing in the albino rat. *Behavior* **22**, 223–244 (1964).
7. Youngentob, S.L., Mozell, M.M., Sheehe, P.R. & Hornung, D.E. A quantitative analysis of sniffing strategies in rats performing odor discrimination tasks. *Physiol. Behav.* **41**, 59–69 (1987).
8. Uchida, N. & Mainen, Z.F. Speed and accuracy of olfactory discrimination in the rat. *Nat. Neurosci.* **6**, 1224–1229 (2003).
9. Vanderwolf, C.H. & Szechtman, H. Electrophysiological correlates of stereotyped sniffing in rats injected with apomorphine. *Pharmacol. Biochem. Behav.* **26**, 299–304 (1987).
10. Kepecs, A., Uchida, N. & Mainen, Z.F. The sniff as a unit of olfactory processing. *Chem. Senses* **31**, 167–179 (2006).
11. Kay, L.M. & Laurent, G. Odor- and context-dependent modulation of mitral cell activity in behaving rats. *Nat. Neurosci.* **2**, 1003–1009 (1999).
12. Sobel, N., Khan, R.M., Hartley, C.A., Sullivan, E.V. & Gabrieli, J.D. Sniffing longer rather than stronger to maintain olfactory detection threshold. *Chem. Senses* **25**, 1–8 (2000).
13. Schoenfeld, T.A. & Cleland, T.A. The anatomical logic of smell. *Trends Neurosci.* **28**, 620–627 (2005).
14. Spors, H., Wachowiak, M., Cohen, L.B. & Friedrich, R.W. Temporal dynamics and latency patterns of receptor neuron input to the olfactory bulb. *J. Neurosci.* **26**, 1247–1259 (2006).
15. Sobel, E.C. & Tank, D.W. Timing of odor stimulation does not alter patterning of olfactory bulb unit activity in freely breathing rats. *J. Neurophysiol.* **69**, 1331–1337 (1993).
16. Adrian, E.D. The role of air movement in olfactory stimulation. *J. Physiol. (Lond.)* **114**, 4–5 (1951).
17. Schoppa, N.E. Synchronization of olfactory bulb mitral cells by precisely timed inhibitory inputs. *Neuron* **49**, 271–283 (2006).
18. Schoppa, N.E. & Westbrook, G.L. Glomerulus-specific synchronization of mitral cells in the olfactory bulb. *Neuron* **31**, 639–651 (2001).
19. Hayar, A., Karnup, S., Shipley, M.T. & Ennis, M. Olfactory bulb glomeruli: external tufted cells intrinsically burst at theta frequency and are entrained by patterned olfactory input. *J. Neurosci.* **24**, 1190–1199 (2004).
20. Chaput, M.A. Respiratory-phase–related coding of olfactory information in the olfactory bulb of awake freely breathing rabbits. *Physiol. Behav.* **36**, 319–324 (1986).
21. Macrides, F. & Chorover, S.L. Olfactory bulb units: activity correlated with inhalation cycles and odor quality. *Science* **175**, 84–87 (1972).
22. Wachowiak, M. & Cohen, L.B. Representation of odorants by receptor neuron input to the mouse olfactory bulb. *Neuron* **32**, 723–735 (2001).
23. Uchida, N., Takahashi, Y.K., Tanifuji, M. & Mori, K. Odor maps in the mammalian olfactory bulb: domain organization and odorant structural features. *Nat. Neurosci.* **3**, 1035–1043 (2000).
24. Yaksi, E. & Friedrich, R.W. Reconstruction of firing rate changes across neuronal populations by temporally deconvolved Ca^{2+} imaging. *Nat. Methods* **3**, 377–383 (2006).
25. Wachowiak, M. *et al.* Inhibition of olfactory receptor neuron input to olfactory bulb glomeruli mediated by suppression of presynaptic calcium influx. *J. Neurophysiol.* **94**, 2700–2712 (2005).
26. Kent, P.F., Mozell, M.M., Murphy, S.J. & Hornung, D.E. The interaction of imposed and inherent olfactory mucosal activity patterns and their composite representation in a mammalian species using voltage-sensitive dyes. *J. Neurosci.* **16**, 345–353 (1996).
27. Johnson, B.A., Woo, C.C. & Leon, M. Spatial coding of odorant features in the glomerular layer of the rat olfactory bulb. *J. Comp. Neurol.* **393**, 457–471 (1998).
28. Macrides, F., Eichenbaum, H.B. & Forbes, W.B. Temporal relationship between sniffing and the limbic theta rhythm during odor discrimination reversal learning. *J. Neurosci.* **2**, 1705–1711 (1982).
29. Zhao, K., Dalton, P., Yang, G.C. & Scherer, P.W. Numerical modeling of turbulent and laminar airflow and odorant transport during sniffing in the human and rat nose. *Chem. Senses* **31**, 107–118 (2006).
30. Duchamp-Viret, P., Duchamp, A. & Chaput, M.A. Peripheral odor coding in the rat and frog: quality and intensity specification. *J. Neurosci.* **20**, 2383–2390 (2000).
31. Reisert, J. & Matthews, H.R. Response properties of isolated mouse olfactory receptor cells. *J. Physiol. (Lond.)* **530**, 113–122 (2001).
32. Wilson, D.A. Habituation of odor responses in the rat anterior piriform cortex. *J. Neurophysiol.* **79**, 1425–1440 (1998).
33. McGann, J.P. *et al.* Odorant representations are modulated by intra- but not interglomerular presynaptic inhibition of olfactory sensory neurons. *Neuron* **48**, 1039–1053 (2005).
34. Hopfield, J.J. Pattern recognition computation using action potential timing for stimulus representation. *Nature* **376**, 33–36 (1995).
35. Margrie, T.W. & Schaefer, A.T. Theta oscillation coupled spike latencies yield computational vigour in a mammalian sensory system. *J. Physiol. (Lond.)* **546**, 363–374 (2003).
36. Pager, J. Respiration and olfactory bulb unit activity in the unrestrained rat: statements and reappraisals. *Behav. Brain Res.* **16**, 81–94 (1985).
37. Bhalla, U.S. & Bower, J.M. Multiday recordings from olfactory bulb neurons in awake freely moving rats: spatially and temporally organized variability in odorant response properties. *J. Comput. Neurosci.* **4**, 221–256 (1997).
38. Schmitt, B.C. & Ache, B.W. Olfaction: responses of a decapod crustacean are enhanced by flicking. *Science* **205**, 204–206 (1979).
39. Kadohisa, M. & Wilson, D.A. Olfactory cortical adaptation facilitates detection of odors against background. *J. Neurophysiol.* **95**, 1888–1896 (2006).
40. Eliades, S.J. & Wang, X. Sensory-motor interaction in the primate auditory cortex during self-initiated vocalizations. *J. Neurophysiol.* **89**, 2194–2207 (2003).
41. Johnson, B.A. & Leon, M. Modular representations of odorants in the glomerular layer of the rat olfactory bulb and the effects of stimulus concentration. *J. Comp. Neurol.* **422**, 496–509 (2000).
42. Linster, C. *et al.* Perceptual correlates of neural representations evoked by odorant enantiomers. *J. Neurosci.* **21**, 9837–9843 (2001).
43. Adrian, E.D. Sensory discrimination with some recent evidence from the olfactory organ. *Br. Med. Bull.* **6**, 330–332 (1950).
44. Katz, D.B., Simon, S.A. & Nicolelis, M.A. Dynamic and multimodal responses of gustatory cortical neurons in awake rats. *J. Neurosci.* **21**, 4478–4489 (2001).
45. Kent, P.F. & Mozell, M.M. The recording of odorant-induced mucosal activity patterns with a voltage-sensitive dye. *J. Neurophysiol.* **68**, 1804–1819 (1992).
46. Tabor, R., Yaksi, E., Weislogel, J.M. & Friedrich, R.W. Processing of odor mixtures in the zebrafish olfactory bulb. *J. Neurosci.* **24**, 6611–6620 (2004).